ISSN: 2414-1895 DOI: 10.6919/ICJE.202505_11(5).0016

Highly-Efficient g-C_3N_4-based Photocatalysts for Radioactive Nuclide Uranium Reduction and Extraction from Water

Die Hu, Sai Zhang*, Kun Xu, and Chengchu Zeng

College of Chemistry and Life Science, Beijing University of Technology, Beijing 100124, China

*zhangsai92@bjut.edu.cn

Abstract

With the continuous growth of global energy demands, the excess utilization of traditional energy sources inevitably causes a series of worldwide problems, incuding resource depletion, environment pollution and climate warming. The separation, enrichment, and extraction of uranium from wastewater and seawater have played an increasingly critical role in development of new green energy and industrial upgrading. Nowadays, the great challenge, which urgently needs to be addressed, is to explore new technology for efficient extraction of radioactive nuclide uranium from water bodies. In recent years, photocatalysis technology for uranium extraction has rapidly developed by reason of its capability for reducing soluble high-valance state uranium (U(VI)) to insoluable low-valance state U(IV), consequently achieving extraction of uranium as well as radioactive wastewater treatment. However, the existed photocatalytic materials still suffer from limitations, such as low reduction rates for U(VI), inhibition effects at ambient environment, lack of research on catalytic mechanism, and practical application barriers. Graphitic carbon nitride (g-C_3N_4), as an emerging two-dimensional layered polymeric semiconductor material, has been regarded as one of the most promising candidates for photocatalytic uranium extraction, owing to its simple synthesis, low cost, strong visible-light absorption, and adjustable electronic band structure. This review systematically introduces the recent advances of g-C_3N_4-based materials in photoreduction, fixation, and extraction of U(VI) from aqueous environments. Also, the processes and reaction mechanisms for typical photocatalytic extraction of U(VI) are presented in detail. Furthermore, the design strategies, U(VI) extraction performance, and advantages/limitations of g-C_3N_4-based photocatalysts are critically evaluated. At length, the future prospects of photocatalytic technology for U(VI) recovery from wastewater and seawater are discussed, highlighting its potential for sustainable energy solutions. This review aims to provide theoretical guidances for the rational design and development of novel photocatalytic materials to purify U(VI)-bearing wastewater and extract radionuclide resources.

Keywords

Photocatalysis; Reduction; Uranium; g-C_3N_4; Mechanism.

1. Introduction

With the gradual increase of global energy consumption, the rapid consumption of non-renewable energy sources (e.g., fossil fuels) has caused severe crises of energy shortages and environmental pollution [1, 2]. The development of sustainable, environmentally benign, and high-quality new energy sources becomes imperative. Nuclear energy, distinguished by its clean and green features, plays an increasingly important role in promoting low-carbon development. Nowadays, the

ISSN: 2414-1895 DOI: 10.6919/ICJE.202505_11(5).0016

exponential growth of nuclear power engineering in worldwide drives a surge in uranium demand [3]. However, terrestrial uranium reserves are finite, and the processes covering uranium mining, fuel processing, as well as spent fuel reprocessing inevitably generate U-containing wastewater [4, 5]. The separation and recovery of uranium from wastewater not only benefits for enhancing utilization efficiency of uranium resource, but also mitigates environmental burdens. Meanwhile, a plenty of uranium (~4.5 billion metric tons) is stored in seawater, which favorably sustains its long-term supply [6]. Despite the enormous potential, uranium extraction from seawater faces serious challenges, including the ultra-low concentrations (~3.3 mg/L), loads of coexisting competitive ions (e.g., Na^+, K^+, Ca^{2+}, and Mg^{2+}), and complex microbial environments [7, 8]. To achieve efficient uranium extraction, multiple physicochemical separation techniques have been explored by researchers worldwide, such as adsorption, chemical reduction, electrocatalysis, membrane separation, and so on [8, 9]. Traditional approaches are usually constrained by complicated synthesis routes, poor environmental anti-interference ability, inferior chemical stability, and low selectivity. By contrast, the reduction and extraction of soluble high-valance state uranium (U(VI)) via photocatalysis can be achieved by utilization of green solar energy, which exhibits exceptional selectivity for dissolved U(VI) species, high recyclability, and significant potential for radioactive wastewater remediation and seawater uranium extraction [10]. To date, multiple photocatalysts have been explored, containing metal oxides, metal sulphides, bismuth-based compounds, layered double hydroxides (LDH), metal-organic frameworks (MOFs), and covalent organic frameworks (COFs) [10, 11]. Nevertheless, the practical application of these photocatalysts remains obstructed by intrinsic limitations, like poor stability, high production costs, and serious secondary pollution. Therefore, developing efficient photocatalysts is the key to implement this technology in practical at large scale.

In recent years, graphitic carbon nitride (g-C_3N_4), as an organic conjugated semiconductor, attracts increasing attention in U(VI) photodegradation and extraction due to visible-light response, physicochemical stability, simple synthesis procedures, low cost, controllable energy level structure, and less secondary pollution [12, 13]. Most previous studies have reported that pristine g-C_3N_4 is commonly synthesized via high temperature thermal polycondensation of nitrogen-rich precursors (e.g., urea, cyanamide, dicyandiamide, melamine, and thiourea) [14, 15]. As shown in Figure 1, basic structure of g-C_3N_4 is composed by s-triazine (C_3N_3) or tri-s-triazine (C_6N_7) units. Moreover, g-C_3N_4 composed of C_6N_7 rings is preferably formed in lower energy and deemed as the most stable configuration at ambient conditions, which was also verified by the first-principle density functional theory (DFT) calculations. Bulk g-C_3N_4 usually suffers from serious drawbacks, such as inefficient utilization of solar energy, low specific surface area, deficient active sites, poor electrical conductivity, and rapid recombination of photogenerated charge carriers, thus hindering its wide application. In general, photocatalytic performances of catalysts mainly depend on their chemical composition, morphological structure, photoelectric properties, light-harvesting capacity, and mass transfer of reactants [8]. Numerous efforts, covering heteroatom doping, construction of heterostructure, morphological control, etc., have been devoted to modifying g-C_3N_4 for suitable electronic energy level, strong light absorption ability, and excellent catalytic performances. As for heteroatom doping, metal or non-metal elements are introduced into skeleton of g-C_3N_4, which resulted in enhanced light absorption and differentiated electronic distribution for better separation of electron-hole (e^--h^+) pairs [16]. Another feasible strategy is fabricating g-C_3N_4-based heterostructure with cocatalysts, including suitable semiconductors, carbonaceous materials, and metal nanoparticles [17]. Through functionalization modification, g-C_3N_4-based materials are endowed with superior photoelectric activity, which offers new methods and materials for immobilization and recovery of U(VI) species from water environment.

Up to now, a number of innovative and meaningful findings on development of g-C_3N_4-based materials have been studied, especially in the past five years. This review systematically summarizes the recent advances of g-C_3N_4-based materials in photoreduction, fixation, and extraction of U(VI) from aqueous environments, discusses the reaction mechanisms and analyzes critical factors for U(VI) photoreduction. Besides, the design strategies, U(VI) extraction performance, and

ISSN: 2414-1895 DOI: 10.6919/ICJE.202505_11(5).0016

advantages/limitations of g-C_3N_4-based photocatalysts are critically evaluated. In the end, an outlook for constructing visible-light-driven g-C_3N_4-based materials on U(VI) removal and enrichment in future is concisely given, and as well highlights its potential for sustainable energy solutions.

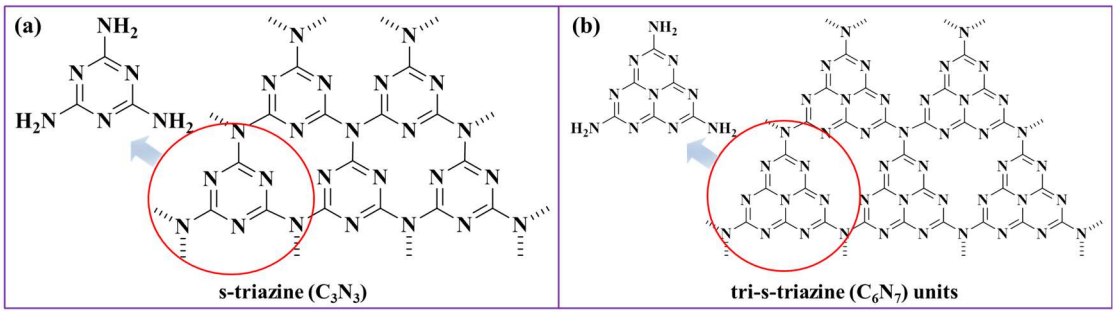

Figure 1. (a) S-triazine and (b) Tri-s-triazine based structures of g-C_3N_4.

2. Principal Mechanism of g-C_3N_4-based Photocatalysts on U(VI) Reduction and Extraction

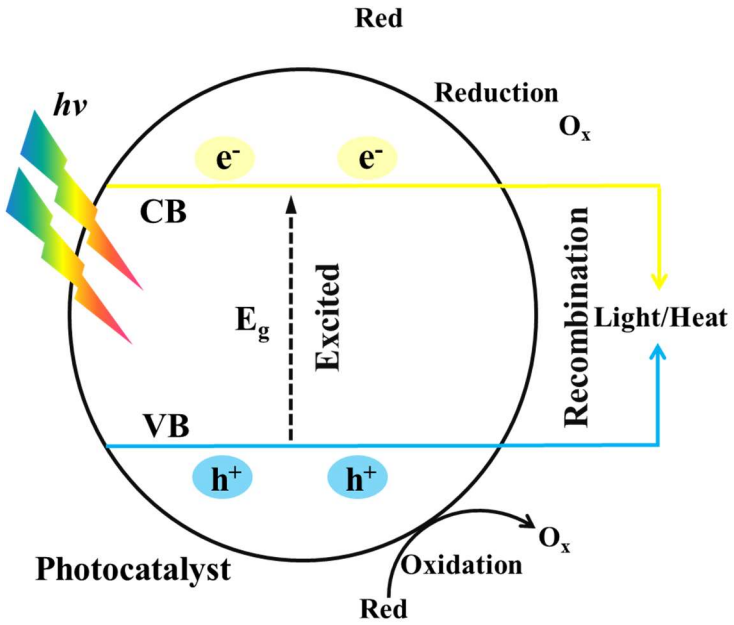

Figure 2. Basic principles of semiconductor photocatalysis with redox reactions.

As a typical n-type semiconductor, photocatalysis mechanisms of g-C_3N_4-based materials obey the heterogeneous catalysis processes. In short, the whole process contains external diffusion of reaction substrates, internal diffusion of reaction substrates, adsorption, surface reaction, desorption, internal diffusion of reaction products, external diffusion of reaction products, respectively [12, 18]. During photocatalysis, catalysts are firstly required to adsorb light, of which the energy value (*hv*) must be equal to or higher than band gap energies (E_g), as shown in Figure 2. Once being excited, photoinduced e^--h^+ pairs are generated, and then e^- in the valence band (VB) **transitioned to** the conduction band (CB) with h^+ concurrently remained on the VB of photocatalysts [19, 20]. Soon afterwards, e^- and h^+ separately migrate to materials surface under the internal electric field（Equation (1)), eventually undergoing redox reactions. Electron acceptors react with photoinduced e^- to generate reduced species, such as $O_2^{\bullet-}$, lower valent metal ions, and so on (Equation (2)). While, electron donors are oxidized by h^+ in reverse during reactions (Equation (3)). However, massive photogenerated e^- and h^+ are undesirably recombined instead of surface reactions, which occurs very

ISSN: 2414-1895 DOI: 10.6919/ICJE.202505_11(5).0016

quickly (90% less than 10 ns) upon excitation [21]. Through this process, the absorbed energy is released as light and heat, thus resulting in inferior photocatalytic performances.

$$\text{Photocatalysts (PC)} + h\nu \rightarrow h^+ \text{(VB)} + e^- \text{(CB)} \quad (1)$$

$$O_x + e^- \text{(CB)} \rightarrow \text{Red} \quad (2)$$

$$\text{Red} + h^+ \text{(VB)} \rightarrow O_x \quad (3)$$

As for U(VI) photoreduction and extraction, different catalytic mechanisms are introduced on basis of reaction atmospheres (e.g., N_2, Ar and air). In general, photoreduction of U(VI) in aqueous solutions are carried out under anaerobic conditions such as N_2, and Ar [22-25]. As previously reported, the transformation of uranium species is quite complex at N_2 atmosphere, while U(VI) is mostly reduced to U(IV) at ultimate under light irradiation [26, 27]. Photoreduction of U(VI) may occur via a two-electron reduction route (Equation (4)) or two-step single-electron transfer process (Equation (5) and Equation (6)). Besides, a disproportionation reaction of U(V) also results in the formation of U(IV) (Equation (7)). Sacrificial agents (e.g., ethanol, benzylalcohol, and methanol) are often required in the system to consume h^+ and prevent the re-oxidation of U(IV), thereby improving photocatalytic activity [22-24].

$$\text{U(VI)} + 2e^- \text{(CB)} \rightarrow \text{U(IV)} \quad (4)$$

$$\text{U(VI)} + e^- \text{(CB)} \rightarrow \text{U(V)} \quad (5)$$

$$\text{U(V)} + e^- \text{(CB)} \rightarrow \text{U(IV)} \quad (6)$$

$$2\text{U(V)} \rightarrow \text{U(IV)} + \text{U(VI)} \quad (7)$$

Based on the above-mentioned mechanisms, the analysis of reduction products mainly is characterized by X-ray photoelectron spectroscopy (XPS) and X-ray absorption fine structure spectroscopy (EXAFS). As for XPS, the changes of characteristic peak intensity and area ratios indirectly confirmed the transformation of U(VI) into U(IV) [28]. While, the peak of U(VI) is also frequently detected after reactions, which is furthered identified by EXAFS. For instance, Fan et al. found that UO_2 precipitation was the main product by EXAFS measurements [29]. Additionally, the fitting results from EXAFS data proved the existence of an extra 2.50 oxygen (O) atoms at R≈ 2.15 Å, which was not attributed to the U-O distance in UO_2 or UO_2^{2+}. This phenomenon probably resulted from the partial oxidation of U(VI)-based products on surface, which was triggered by dissolved O_2 in water, h^+ and reactive oxygen species generated during photocatalysis, or O_2 in air [30].

Along with the in-depth study of catalytic mechanism, O_2 is also found helpful for U(VI) photoreduction. In the photocatalysis process involving O_2 and H_2O, four typical reactive oxidative species are usually formed, containing hydrogen peroxide (H_2O_2), superoxide radicals ($O_2^{\bullet-}$), hydroxyl radicals ($^{\bullet}OH$), and singlet oxygen ($^1O_2$). For a certain reaction systems, $O_2^{\bullet-}$ is favorable and can directly reduce U(VI) into U(IV) as followed (Equation (8) and Equation (9)). For example, a novel polypyrrole modified carbon nitride (PPy/CN) composite was designed and prepared for U(IV) photoreduction at ambient conditions [28]. With the solution pH= 6.0 and initial concentration of 40 mg/L, U(VI) was completely reduced into U(IV) within 20 min. The superior photocatalytic activity was attributed to $O_2^{\bullet-}$, which was yielded from reduction of dissolved O_2 by photoelectrons and then

ISSN: 2414-1895 DOI: 10.6919/ICJE.202505_11(5).0016

reacted with UO_2^{2+} to form solid UO_2. Effective photoreduction and extraction of U(IV) in ambient environment benefits for practical application and technology promotion at a large scale.

$$O_2 + e^- (CB) \rightarrow O_2^{\bullet-} \quad (8)$$

$$2O_2^{\bullet-} + UO_2^{2+} \rightarrow UO_2 + 2O_2 \quad (9)$$

3. Advancements in the Application of g-C_3N_4-based Photocatalysts on U(VI) Reduction and Extraction

Considering the poor utilization of visible light and low quantum efficiency for primary g-C_3N_4, many strategies on optimizing g-C_3N_4-based photocatalysts are proposed, covering heteroatom doping, construction of heterostructure, and so on. In the past few years, heteroatom doping is treated as an effective method on modifying g-C_3N_4 to overcome the limitations for U(VI) photoreduction, during which the introduction of metal/non-metal elements into g-C_3N_4 framework may adjust the bandgap with suitable energy levels and improve its visible light absorption capability. For instance, Hong and co-workers successfully prepared metallic Fe doping g-C_3N_4 by a one-step pyrolysis strategy for U(VI) photoreduction [31]. As shown in Figure 3a and b, Fe was firmly embedded into conjugated aromatic heterocycles by forming Fe-N_x configurations, which served as predominant reactive sites to bind U(VI) species, and photogenerated electrons favorably transferred to g-C_3N_4 surface with efficient charge separation. The reduction efficiency of U(VI) could reach 99% with a reaction rate constant of 0.091 min^{-1}, approximately ~9 times faster than that of pure g-C_3N_4, demonstrating the importance of Fe doping for promoting U(VI) photoreduction. To reduce costs and enhance stability, Lu et al. and Wu et al. proposed to functionalize g-C_3N_4 by non-metal elements boron (B) or sulfur (S) doping for efficient U(VI) photoreduction, respectively [32, 33]. As shown in Figure 3c, CS_2 was selected as sulfur source to obtain S-g-C_3N_4 and S atoms were evidenced to substitute the lattice N of g-C_3N_4 by forming C-S and C-SO_x-C bond [32]. Through DFT calculations (Figure 3d), it was found that S-C bonds (1.62-1.84 Å) were much longer than N-C bonds (1.35-1.46 Å), which meant the extension of melem units and thus favored the bonding of U(VI) ions on S-g-C_3N_4 surface. The S doping rationally regulated the electronic structure of g-C_3N_4 with suitable energy levels as well as good charge separation, resulting in efficient reduction of U(VI) with high activity and stability. While, P doped g-C_3N_4 ($P_3C_3N_4$) was prepared by using butyl phosphate and urea as P source and precursor, respectively [33]. Unexpectedly, P preferentially replaced C atoms in aromatic heterocycles of g-C_3N_4, thus resulting in a narrowed band gap, promoted light absorption and accelerated charge transfer. After 20 min reaction under visible light, ~90% of U(VI) was reduced over $P_3C_3N_4$ (Figure 3e), which was much higher than that of pure g-C_3N_4 (~40%).

In order to further boost the photoreduction and extraction of U(VI) from water environment, the co-doping strategy is also put forward to precisely regulate properties of g-C_3N_4. For example, Zhang and co-workers synthesized a non-metal O, P co-doped g-C_3N_4 (OPCN) by a facile one-step thermal polycondensation route with melamine phosphate and melamine as raw materials [34]. After doping O and P atoms, the band gap value of CN reduced from 2.62 eV to 2.51~2.55 eV (OPCN-1~OPCN-3), which promoted U(VI) photoreduction with an sharply increased efficiency of 94.9% upon illuminated by a white LED. Through mechanism analysis, it could be found that UO_2^{2+} in solution was eventually transformed to peroxides $(UO_2)O_2 \cdot 2H_2O$ by reacting with $O_2^{\bullet-}$, while a part of UO_2^{2+} species were first reduced by photoelectrons to generate UO_2 (s) intermediates. Furthermore, Zhang et al. successively introduced Fe, P and O into original g-C_3N_4 skeleton (OPFCN) by a one-pot thermal condensation synthesis, during which melamine, ferric nitrate nonahydrate, hexachlorotriphosphazene, and polyvinylpyrrolidone were chosen as precursor and doping sources (for Fe, P, and O doping, respectively). Combined quenching experiments and EPR measurement results, it could be inferred that the U(VI) photoreduction majorly depended on electrons, which transferred from P and O atoms to adjacent atoms for extending the π delocalized conjugation in g-

ISSN: 2414-1895 DOI: 10.6919/ICJE.202505_11(5).0016

C_3N_4 and then accumulated around Fe atoms via coordination bonding. Due to efficient charge separation and high light quantum efficiency, the reduction efficiency of U(VI) over OPFCN was significantly increased to 98.7% by contrast to pure CN (24.5%) in 300 min, and the relevant kinetic constant of OPFCN was 30.8 times higher than pure CN. The above findings undoubtedly confirmed the availability of doping on functionalizing g-C_3N_4-based photocatalysts towards U(VI) photoreduction and enrichment from radioactive wastewater or seawater.

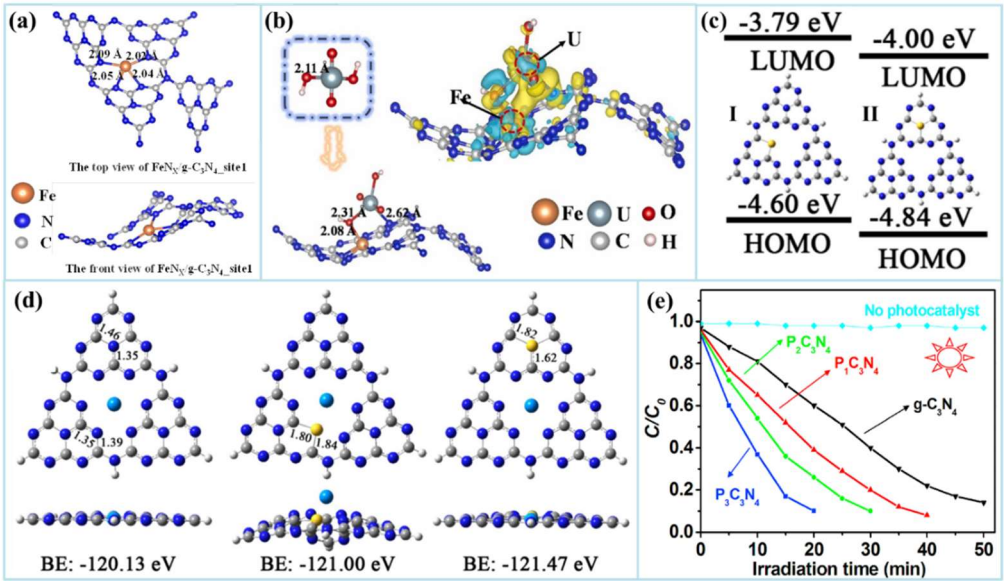

Figure 3. (a) The optimized structures for Fe doping g-C_3N_4 with Fe occupying site1, and (b) the charge density difference of the most stable configuration of $UO_2(OH)_2$ adsorped onto FeN_x/g-C_3N_4 [31]; (c) Molecular orbital energies and structures of the g-C_3N_4 and S-g-C_3N_4, and (d) the coordination complexes with U(VI) ion (Blue, gray, yellow, and cyan ball represents C, N, S and U(VI), respectively) [32]; (e) Photoreduction performances of UO_2^{2+} over different samples [33].

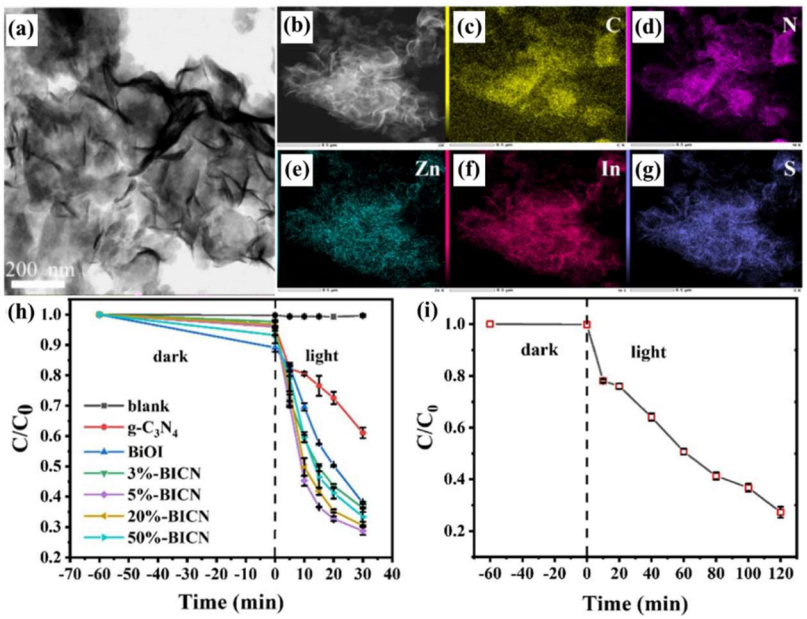

Figure 4. (a, b) TEM image, and TEM-EDX elemental mapping images of (c) C, (d) N, (e) Zn, (f) In and (g) S of ZISCN-2 [35]; (h) Photocatalytic reduction of different composites (C_0= 60 mg/L, s/l= 0.5 g/L, pH= 5.0), and (i) photocatalytic performance of 5%-BICN composite (C_0= 300 mg/L, 10 mg catalysts, pH= 5.0) [38].

ISSN: 2414-1895 DOI: 10.6919/ICJE.202505_11(5).0016

Except for heteroatom doping, the construction of heterostructure is another promising strategy for functionalization of g-C_3N_4, which is usually coupled with noble/non-noble metal nanoparticles (e.g., Ag, Au, Pt, Pd and Ni), appropriate semiconductor (e.g., TiO_2, CeO_2, and $AgPO_4$), and carbonaceous nanomaterials (e.g., carbon nanotubes, reduced graphene oxides, and fullerene). Constructing heterostructure is an excellent method for forming the coherent interface, building internal electric field, and enhancing electric conductivity. Dai et al. designed and fabricated an effective S-scheme heterojunction photocatalyst by in-situ growing $ZnIn_2S_4$ onto g-C_3N_4 surface (ZISCN) [35]. As shown in Figure 4a-g, a typical lamellar structure was obtained for the optimal ZISCN-2 with homogeneous distribution of C, N, S, In and Zn elements. An internal electric field was constructed at the heterojunction interface between $ZnIn_2S_4$ and g-C_3N_4 to promote charge separation and transfer, and as well the visible light absorption was also enhanced. Thus, the U(VI) photoreduction was achieved at ambient environment without sacrificial agents added, of which the efficiency reached ~85% in 300 min reaction time and obviously surpassed that of individual g-C_3N_4 (~10%) and $ZnIn_2S_4$ (~25%). Consequently, U(VI) species were transformed into $(UO_2)O_2{\cdot}2H_2O$ precipitation by reacting with $O_2^{\bullet-}/H_2O_2$ in the photocatalytic system. Later on, He et al. developed a photoactive CdS/g-C_3N_4 cellulose membrane (CCM) by decorating CdS/g-C_3N_4 powders onto the collodion cellulose [36]. The desired CCM composites exhibited a macro structure with uniform distribution of reactive centers, which improved charge carriers migration in bulk and accelerated mass transfer during reactions, hence benefiting for sacrificial-agent-free U(VI) reduction and extraction at air atmosphere. Upon being illuminated by a 350 W Xe lamp, ~95% of U(VI) could be reduced and the extraction capacity was increased up to ~1599.72 mg/g, displaying a great potential on separation of uranium from solutions.

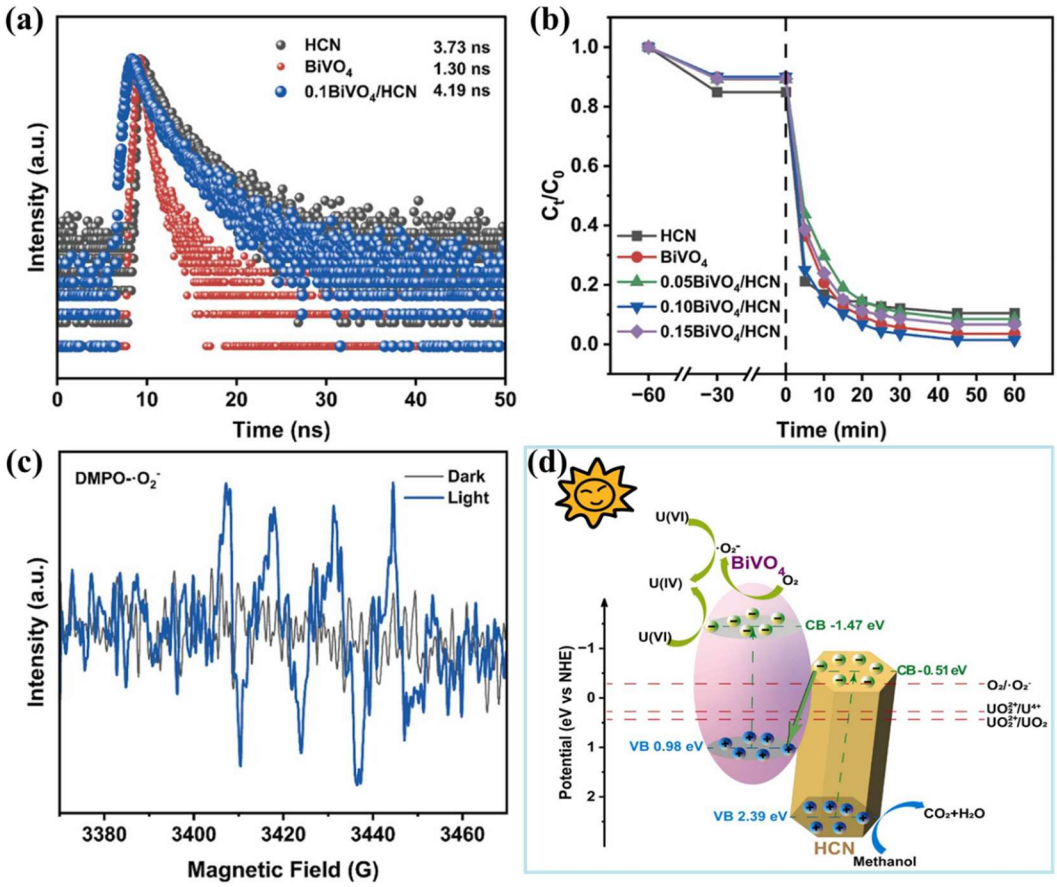

Figure 5. (a) Fluorescence lifetime decay curves of 0.10 $BiVO_4$/HCN, $BiVO_4$, and HCN; (b) The photoreduction activities of U(VI) over different catalysts; (c) ESR spectra of DMPO-$O_2^{\bullet-}$ under illumination or in the dark; (d) Mechanism diagram for U(VI) photoreduction over $BiVO_4$/HCN [39].

ISSN: 2414-1895 DOI: 10.6919/ICJE.202505_11(5).0016

Apart from metal sulfides, bismuth (Bi) based semiconductors were also good candidates to couple with g-C_3N_4 for property modulation and catalytic activity improvement [37-39]. In one pioneer study, BiOI/g-C_3N_4 (BICN) composites were obtained by a combined high-temperature calcination and hydrothermal route, followed by U(VI) photoreduction tests [38]. During synthesis, g-C_3N_4 was firstly prepared via thermal condensation of melamine, and then was served as supporter for the growth of BiOI using hydrothermal synthesis, eventually leading to the formation of heterojunction in BICN composites. By compared with individual g-C_3N_4 and BiOI, 5%-BICN displayed greater photocurrent density and lower internal resistance, suggesting a better photoelectric behavior. Batch experiments revealed that 5%-BICN exhibited an exceptional capability for U(VI) reduction (Figure 4h and i), of which the photocatalytic performance improved ~3.0 and 1.5 times over g-C_3N_4 and BiOI with U(VI) concentration of 60 mg/L, respectively. Analyzed by various characterizations, an enhanced separation and migration of photoinduced carriers were achieved for BICN composites, which obviously contributed to the production of $O_2^{\bullet-}$ radicals and were responsible for U(VI) photoreduction. Instead of BiOI, Li et al. fabricated a Z-scheme bismuth vanadate/hydrothermal carbon nitride ($BiVO_4$/HCN) composite via a similar hydrothermal process, where the shaped CN required a direct annealing pretreatment [39]. The Z-Scheme heterojunction between HCN and $BiVO_4$ resulted in the generation of an internal electric field, and the robust interfacial connection could serve as bridge to boost charge carriers separation. Therefore, a longer average carriers lifetime was achieved for 0.10 $BiVO_4$/HCN (4.19 ns) than single HCN (3.73 ns) and $BiVO_4$ (1.30 ns), as shown in Figure 5a. With the optimal $BiVO_4$ content (10% relative to mass of CN), 0.10 $BiVO_4$/HCN owned a best photocatalytic behavior and could reduce 98.5% of U(VI) within 45 min irradiated by λ> 420 nm visible light (Figure 5b). Integrating quenching experiments, ESR spectra with XPS measurements, a possible Z-scheme electron transfer mechanism was proposed that photoinduced e^- on the CB of $BiVO_4$ directly reduced U(VI) to (IV), and as well reacted with O_2 to yield $O_2^{\bullet-}$ for subsequent reduction of U(VI), while h^+ left on HCN was sacrificed by methanol (Figure 5c and d). Diversified g-C_3N_4-based heterostructure composites have been developed to utilize green solar energy for uranium enrichment from water bodies [14, 15].

Over the past few years, many efforts have been devoted to exploring effective modification strategies and excellent visible-light-driven g-C_3N_4-based materials, covering donor-acceptor-type hollow g-C_3N_4 heterojunction (PTPS@HCN) [40], carboxyl groups functionzed g-C_3N_4 (CCN) [41], P-doped tubular g-C_3N_4 (P-TCN) [42], Ni-anchored S-doped g-C_3N_4/RGO (Ni-SCN@G) [43], tubular LDHS@TCN composites [44], Fe_3O_4/g-C_3N_4 [45], Fe_3O_4/GO/g-C_3N_4 [46], carbon-dots-modified porous g-C_3N_4 (CNCD) [47], for uranium reduction and extraction.

4. Summary and Future Perspectives

To summarize, the extraction and reduction of uranium from water environments is a crucial issue for the global energy transition and environmental protection. On basis of recent researches, substantial progress has been made in this field, especially for photocatalysis technology, among which visible-light-response g-C_3N_4-based photocatalysts attract increasingly widespread attention and exhibits great potential on uranium reduction and extraction from water environments. Generally speaking, the urgent desire for g-C_3N_4 mostly depends on optimization of its photocatalytic activity and stability, as well as the potential applications. To improve the photocatalytic performances, lots of efforts are devoted on designing and exploring functionalization methods to develop highly efficient g-C_3N_4-based photocatalysts in the past few years, which possess exceptional opto-electronic properties and chemical characteristics. This review gives a clarification on photoreduction mechanism of soluable uranium species with high valence, and retrospects the recent advances in modifying g-C_3N_4 via heteroatom doping and fabricating heterostructure for better catalytic performances. Through forming internal electric field, heterojunctions or unique architectures, the significantly enhanced photocatalytic activity for g-C_3N_4-based photocatalysts is realized, which is probably originated from good visible light absorption, strong reduction ability, high chemical stability, and potential value in large-scale practical application.

ISSN: 2414-1895 DOI: 10.6919/ICJE.202505_11(5).0016

However, numerous challenges and opportunities persist in the field:

(1) To extract uranium from water bodies via photocatalysis, sacrificial agents are usually required to consume strong oxidized photogenerated h^+ and anaerobic environment need to be supplied in most cases, thus hindering its long-term use and large-scale application.

(2) For efficient U(VI) photoreduction and extraction, a deeper understanding of charge carriers transfer paths should be unveiled and analyzed through multiple characterization techniques, and also theoretical calculations are needed to predict reduction processes, especially for complex water environment.

(3) Most photocatalysts are limited by high synthesis cost, lack of active sites, poor light utilization, and low surface reaction efficiency, causing difficulty on industrial applications promotion.

In view of green solar energy-driven strategies, the frontier research can focus on design and development of novel photocatalysts via facile and low-cost method. And also, new materials should be endowed with excellent light absorption, faster charge carriers transfer, high light quantum efficiency, stronger capture capacities and significantly promoted reaction kinetics, thereby achieving efficient uranium photoreduction and extraction for promising practical applications.

Acknowledgments

We gratefully acknowledge funding support from the National Natural Science Foundation of China (Grant Nos. 22106047).

References

[1] Monnet, A.;Gabriel, S; Percebois, J. Analysis of the long-term availability of uranium: The influence of dynamic constraints and market competition. Energy Policy. 2017, 105, 98-107.

[2] Dong, D.; Guan, J.Y.; Wang, Z.Q.; Wang, Y.Q. Current status and trends of nuclear energy under carbon neutrality conditions in China. Energy. 2025, 314, 134253.

[3] Fernández-Arias, P.; Lampropoulos, G.; Antón-Sancho, Á.; Vergara, D. Progress, Challenges, and Sustainable Perspectives in Nuclear Energy Strategies. Applied Sciences. 2024, 14, 11864.

[4] Zhu, Y.S.; Chen, S.S; Li, Z.M; Shaban, M.; Chen, C.L. Nanoscale zero-valent iron composites for uranium-contaminated water treatment and environmental remediation: a review. Environmental Science: Nano. 2025, 12, 20-40.

[5] Mei, D.C.; Liu, L.J.; Yan, B. Adsorption of uranium (VI) by metal-organic frameworks and covalent-organic frameworks from water. Coordination Chemistry Reviews. 2023, 475, 214917.

[6] Xie, Y.; Liu, Z.Y.; Geng, Y.Y.; Li, H; Wang, N.; Song, Y.P.; Wang, X.L.; Chen, J.; Wang, J.C.; Ma, S.Q.; Ye, G. Uranium extraction from seawater: material design, emerging technologies and marine engineering. Chemical Society Reviews. 2023, 52, 97-162.

[7] Wei, W.; Luo, J.Q.; Liu, S.J.; Zhou, Y.M.; Ma, J.G. Enhancing the photocatalytic performance of g-C3N4 by using iron single-atom doping for the reduction of U(VI) in aqueous solutions. Journal of Solid State Chemistry. 2022, 312, 123160.

[8] Zhang, D.; Fang, L.; Liu, L.J.; Zhao, B.; Hu, B.W.; Yu, S.J.; Wang, X.K. Uranium extraction from seawater by novel materials: A review. Separation and Purification Technology. 2023, 320, 124204.

[9] Zhu, J.H.; Wang, J.; Liu, Q.; Yu, J.; Liu, J.Y.; Chen, R.R.; Song, D.L.; Li, R.M.; Wang, J. Advanced MXene-based materials for efficient extraction of uranium from seawater and wastewater. Science of The Total Environment. 2024, 942, 173755.

[10] Ighalo, J.O.; Chen, Z.H.; Ohoro, C.R.; Oniye, M.; Igwegbe, C.A.; Elimhingbovo, I.; Khongthaw, B.; Dulta, K.; Yap, P.; Anastopoulos, I. A review of remediation technologies for uranium-contaminated water. Chemosphere. 2024, 352, 141322.

[11] Dai, Z.R.; Chen, L.J.; Zhang, W.L.; Liang, B.C.; Gao, Y.; Li, L. K doped defective g-C3N4 decorated with cyano group for boosting visible-light driven photocatalytic removal of uranium. Separation and Purification Technology. 2024, 338, 126537.

ISSN: 2414-1895 DOI: 10.6919/ICJE.202505_11(5).0016

[12] Mamba, G.; Mishra, A.K. Graphitic carbon nitride (g-C3N4) nanocomposites: A new and exciting generation of visible light driven photocatalysts for environmental pollution remediation. Applied Catalysis B: Environmental. 2016, 198, 347-377.

[13] Zhang, S.; Gu, P.C.; Ma, R.; Luo, C.T.; Wen, T.; Zhao, G.X.; Cheng, W.C.; Wang, X.K. Recent developments in fabrication and structure regulation of visible-light-driven g-C3N4-based photocatalysts towards water purification: A critical review. Catalysis Today. 2019, 335, 65-77.

[14] Ye, Y.; Jin, J; Chen, F.; Dionysiou, D.D.; Feng, Y.Y.; Liang, B.; Cheng, H.Y.; Qin, Z.M.; Tang, X.; Li, H.W.; Yntema, D.; Li, C.; Chen, Y.L.; Wang, Y.H. Removal and recovery of aqueous U(VI) by heterogeneous photocatalysis: Progress and challenges. Chemical Engineering Journal. 2022, 450, 138317.

[15] Liu, C.L.; Guo, Y.D.; Li, S.H.; Xuan, K.; Guo, Y.P.; Li, J.; Wang, X.G.; Li, X.M.; Zhou, Z.K. Mesoporous sulfur-doped g-C3N4@attapulgite composite as an advanced photocatalyst for efficiently uranium(VI) recovery from aqueous solutions. Journal of Environmental Chemical Engineering. 2024, 12, 112886.

[16] Zhu, W.Y.; Yue, Y.X.; Wang, H.H.; Zhang, B.; Hou, R.B.; Xiao, J.T.; Huang, X.S.; Ishag, A.; Sun, Y.B. Recent advances on energy and environmental application of graphitic carbon nitride (g-C3N4)-based photocatalysts: A review. Journal of Environmental Chemical Engineering. 2023, 11, 110164.

[17] Li, S.T.; Wang, Y.; Wang, J.J.; Liang, J.J.; Li, Y.Q.; Li, P. Modifying g-C3N4 with oxidized Ti3C2 MXene for boosting photocatalytic U(VI) reduction performance. Journal of Molecular Liquids. 2022, 346, 117937.

[18] Zhang, S.; Chen, L.X.; Qu, Z.Y.; Zhai, F.W., Yin, X.X.; Zhang, D.; Shen, Y.F.; Li, H.; Liu, W.; Mei, S.; Ji, G.X.; Zhang, C.; Dai, X.; Chai, A.F.; Wang, S.A. Confining Ti-oxo clusters in covalent organic framework micropores for photocatalytic reduction of the dominant uranium species in seawater. Chem. 2023, 9, 3172-3184.

[19] Chen, L.J.; Gao, Y.; Lian, J.J.; Li, L.; Ding, D.X.; Dai, Z.R. Efficient photoreduction removal of uranium(VI) by O, K co-doped g-C3N4 under air atmosphere without sacrificial agents. Separation and Purification Technology. 2023, 307, 122873.

[20] Gong, Y.; Li, H.K.; Jiao, C.; Xu, Q.C.; Xu, X.Y.; Zhang, X.M.; Liu, Y.F.; Dai, Z.Y.; Liu, X.Y.; Chen, W.; Liu, L.; Zhan, D. Effective hydrogenation of g-C3N4 for enhanced photocatalytic performance revealed by molecular structure dynamics. Applied Catalysis B: Environmental. 2019, 250, 63-70.

[21] Vale, B.R.C.; Scolfaro, D.; Sousa, C.A.; Fonseca, A.F.V.; Bonato, L.G.; Nogueira, A.F.; Bettini, J.; Padilha, L.A. Charge trapping and detrapping in CsPbBr3 perovskite nanocrystals: Implications for photovoltaic and photocatalysis applications. ACS Applied Nano Materials. 2025, 8, 4373-4383.

[22] Song, Z.K.; Yan, C.P.; Qiu, J.L.; Liu, C.; Zhu, Y.A.; Wang, B.; Xie, Z.B.; Chen, G.; Li, K.Q.; Le, Z.G. Photocatalytic reduction of the uranium(VI) by ultra-thin porous g-C3N4 nanosheets synthesized via microwave-assisted. Journal of Environmental Chemical Engineering. 2024, 12, 113951.

[23] Yu, J.Q.; Zhang, H.S.; Liu, Q.; Yu, J.; Zhu, J.H.; Li, R.M.; Liu, P.L.; Li, Y.; Wang, J. Antibacterial AO-CS/CdS-porous few-layer g-C3N4 nanofiber membrane for high-efficiency uranium extraction from seawater: A dual adsorption-photocatalytic regulation strategy. Chemical Engineering Journal. 2023, 471, 144705.

[24] Zhang, L.Y.; Yang, Y.H.; Zhao, N.; Liu, S.; Wang, Z.; Wang, X.K.; Lu, Y.X.; MOF-modified C3N4 for efficient photo-induced removal of uranium under air without sacrificial agents. Journal of Materials Chemistry A. 2024, 12, 9651-9660.

[25] Wang, J.J.; Wang, Y.; Wang, W.; Peng, T.; Liang, J.J.; Li, P.; Pan, D.Q.; Fan, Q.H.; Wu, W.S. Visible light driven Ti3+ self-doped TiO2 for adsorption-photocatalysis of aqueous U(VI). Environmental Pollution. 2020, 262, 114373.

[26] Liu, Y.L.; Gao, Y.; Chen, L.J.; Li, L.; Ding, D.X.; Dai, Z.R. MnOx-decorated oxygen-doped g-C3N4 with enhanced photocatalytic activity for efficient removal of uranium(VI). Separation and Purification Technology. 2023, 307, 122794.

[27] Yu, K.F.; Li, Y.; Cao, X.; Wang, R.X.; Zhou, L.; Wu, L.Z.; He, N.N.; Lei, J.; Fu, D.J.; Chen, T.; He, R.; Zhu, W.K. In-situ constructing amidoxime groups on metal-free g-C3N4 to enhance chemisorption, light absorption, and carrier separation for efficient photo-assisted uranium(VI) extraction. Journal of Hazardous Materials. 2023, 460, 132356.

ISSN: 2414-1895 DOI: 10.6919/ICJE.202505_11(5).0016

[28] Xue, J.M.; Xie, Z.B.; Wang, B.; Zhu, Y.A.; Wu, Z.W.; Nie, Y.D.; Le, Z.G. Enhanced visible-light photocatalytic performance by PPy/CN composites for reduction of UO22+. Journal of Solid State Chemistry. 2022, 315, 123440.

[29] Wang, J.J.; Wang, Y.; Wang, W.; Ding, Z.; Geng, R.Y.; Li, P.; Pan, D.Q.; Liang, J.J.; Qin, H.B.; Fan, Q.H. Tunable mesoporous g-C3N4 nanosheets as a metal-free catalyst for enhanced visible-light-driven photocatalytic reduction of U(VI). Chemical Engineering Journal. 2020, 383, 123193.

[30] Cantrell K.J.; Kaplan D.I.; Wietsma T.W. Zero-valent iron for the in situ remediation of selected metals in groundwater. Journal of Hazardous Materials. 1995, 42, 201-212.

[31] Hong, J.H.; Ma, R.; Wu, Y.C.; Liu, Y.; Wen, T.; Zhang, S.; Wang, S.H.; Wang, X.K.; Ai, Y.J. Experimental and theoretical identifications of durable Fe–Nx configurations embedded in graphitic carbon nitride for uranium photoreduction. Journal of Environmental Chemical Engineering. 2022, 10, 108374.

[32] Lu, C.H.; Zhang, P.; Jiang, S.J.; Wu, X.; Song, S.Q.; Zhu, M.S.; Lou, Z.Z.; Li, Z.; Liu, F.; Liu, Y.H.; Wang, Y.; Le, Z.G. Photocatalytic reduction elimination of UO22+ pollutant under visible light with metal-free sulfur doped g-C3N4 photocatalyst. Applied Catalysis B: Environmental. 2017, 200, 378-385.

[33] Wu, X.; Jiang, S.J.; Song, S.Q.; Sun, C.Z. Constructing effective photocatalytic purification system with P-introduced g-C3N4 for elimination of UO22+. Applied Surface Science. 2018, 430, 371-379.

[34] Zhang, G.Z.; Lei, T.; Wang, D.D.; Tian, X.D.; Wang, Y.; Yang, W.T.; Xu, Q.; Su, Z.M. One-step synthesis of O, P co-doped g-C3N4 under air for photocatalytic reduction of uranium. Journal of Solid State Chemistry. 2024, 339, 124941.

[35] Dai Z.R.; Liang, B.C.; Chen, L.J.; Zhang, W.L.; Gao, Y.; Li, L. Rational construction of S-scheme ZnIn2S4/g-C3N4 heterojunction for effective sacrificial agent-free uranium photocatalysis in air. Separation and Purification Technology. 2025, 354, 129241.

[36] He, T.; Wang Y.; An, M.Y.; Ji, M.B.; Liu, P.; Li, Peng. The photocatalytic extraction of U(VI) by CdS/g-C3N4 cellulose film. Journal of Molecular Liquids. 2024, 395, 123851.

[37] Zhang, X.; Yuan, X.Z.; Jiang, L.B.; Zhang, J.; Yu, H.B.; Wang, H.; Zeng, G.M. Powerful combination of 2D g-C3N4 and 2D nanomaterials for photocatalysis: Recent advances. Chemical Engineering Journal. 2020, 390, 124475.

[38] Xiao, Y.J.; Chen, S.; Li, P.; Zhang, D.; Wang, J.J.; Dong, H.; He, Y.R. Photocatalytic removal of U(VI) from aqueous solution under visible light by bismuth oxyiodide/graphitic carbon nitride composite. Journal of Colloid and Interface Science. 2025, 684, 131-139.

[39] Qiu, J.L.; Zhu, Y.A.; Wang, B.; Nie, Y.D.; Song, Z.K.; Li, P.; Xie, Z.B.; Le, Z.G. Enhanced removal of aqueous uranium: Photocatalytic U(VI) reduction over bismuth vanadate/hydrothermal carbon nitride under visible light. Journal of Environmental Chemical Engineering. 2025, 13, 115009.

[40] Hou, G.L., Dong, W.J.; Li, Z.F.; Cao, X.H.; Zou, L.X.; Liu, Y.H.; Zhang, Z.B. Donor-acceptor characteristic g-C3N4 hollow nanospheres heterojunctions for efficient photocatalytic uranium reduction. Journal of Solid State Chemistry. 2024, 336, 124739.

[41] Li, P.; Wang, Y.; Wang, J.J.; Dong, L.; Zhang, W.T.; Lu, Z.H.; Liang, J.J.; Pan, D.Q., Fan, Q.H. Carboxyl groups on g-C3N4 for boosting the photocatalytic U(VI) reduction in the presence of carbonates. Chemical Engineering Journal. 2021, 414, 128810.

[42] Guo, S.E.; Deng, Z.P.; Li, M.X.; Jiang, B.J.; Tian, C.G.; Pan, Q.J.; Fu, H.G. Phosphorus-doped carbon nitride tubes with a layered micro-nanostructure for enhanced visible-light photocatalytic hydrogen evolution. Angewandte Chemie International Edition. 2016, 55, 1830-1834.

[43] Wang, W.; Luo, Q.; Li, L.Q.; Wang, Y.F.; Huo, X.B.; Chen, S.P.; Du, X.W.; Wang, N. Ni-single-atom mediated 2d heterostructures for highly efficient uranyl photoreduction. Advanced Functional Materials. 2023, 33, 2302913.

[44] Liu, N.; Li, R.M.; Song, D.L.; Liu, Q.; Zhu, J.H.; Yu, J.; Li, Y.; Zhang, H.S.; Wang, J. Tubular LDHS@TCN composites for photo-assisted uranium extraction. Progress in Nuclear Energy. 2023, 165, 104910.

[45] Zhang, X.Y.; Wang, J.J.; Li, P.; Xiao, Y.J.; Tan, Z.Y.; He, Y.R.; Habibul, N.; Removal of U(VI) from aqueous solution via photoreduction over Fe3O4/g-C3N4 composite under visible light irradiation. Journal of Hazardous Materials Advances. 2021, 3, 100017.

ISSN: 2414-1895 DOI: 10.6919/ICJE.202505_11(5).0016

[46] Bao, L.F.; Han, J.J.; Wang, H.F.; Liu, R.R.; Qiu, M.Q.; Hu, B.W. High efficient photoreduction of U(VI) by a new synergistic photocatalyst of Fe3O4 nanoparticle on GO/g-C3N4 composites. Journal of Materials Research and Technology. 2022, 18, 4248-4255.

[47] Dai, Z.R.; Zhao, S.; Lian, J.J.; Li, L.; Ding, D.X. Efficient visible-light-driven photoreduction of U(VI) by carbon dots modified porous g-C3N4. Separation and Purification Technology. 2022, 298, 121590.